Effects of Shallow Bi-Angle, Thin-Ply Laminates on the Structural Performance of Composite Wings

Yong Han Noel Kim

A thesis
submitted in partial fulfillment of the
requirements for the degree of

Master of Science

University of Washington

2016

Reading Committee:

Jinkyu Yang, Chair

Marco Salviato

Program Authorized to Offer Degree:
Department of Aeronautics and Astronautics

University of Washington

Abstract

Effects of Shallow Bi-Angle, Thin-Ply Laminates on the Structural Performance of Composite Wings

Yong Han Noel Kim

Chair of the Supervisory Committee:
Professor Jinkyu Yang
Department of Aeronautics and Astronautics Engineering

In this study, we investigate the enhancement of mechanical properties that *shallow bi-angle, thin-ply* laminates bring to fiber reinforced polymer composites. Coupon- and structural-level tests are conducted along with numerical simulations. According to the coupon tests, we find that shallow bi-angle fibers and thin plies can increase the axial stiffness of laminates significantly at the cost of relatively small decrease in their transverse and shear moduli. For the structural tests, we fabricate composite wing structures using an out-of-autoclave vacuum assisted resin transfer molding process. By conducting static bending tests, we show superior structural performances of the wing structure that employs shallow bi-angle fibers and thin-ply fabric, compared to those that use conventional fiber-angle and thick plies. Shallow bi-angle and thin-ply technologies can open new routes to designing composite structures with improved stiffness and strength with fast and cost-effective fabrication processes.

Table of Contents

Chapter 1

Introduction

Carbon fiber reinforced plastic (CFRP) is a type of advanced composite, in which carbon fibers are embedded in a polymeric matrix material that holds the fibers together to form a material system capable of carrying loads [1]. These CFRP composites are particularly useful for aerospace structures due to their superb mechanical properties, such as lightweight, high strength, and durability against harsh environments. CFRP also holds a great advantage over other homogeneous materials for its tailorable mechanical properties. This tailoring capability is achieved by orienting fibers in optimized directions. However, current industry practice recommends the use of limited fiber orientations in 0°, 90°, and $\pm 45^\circ$ fiber angles, and laminate properties are controlled by varying the ratios of these four angles [2]. Furthermore, the *black aluminum* design rule has been widely adopted, in which we employ the equal amount of 0°, 90°, and $\pm 45^\circ$ plies in CFRP composites [3]. This black aluminum approach, however, suppresses the inherent merit of CFRP composites, particularly the aforementioned tailorable nature and the design freedom of composites. In an aerospace wing structure, for example, the primary stresses developed under bending are tension or compression along the wing span direction, and there is no need to allocate a large amount of materials to the transverse-direction as guided by the black aluminum rule. Similarly, in a fuselage structure, hoop stresses are ideally twice larger than the stresses in

the longitudinal direction of the fuselage. Thus, the usage of the black aluminum approach will dilute the tailorable advantage of the CFRP composites.

In this study, we explore an alternative composite design approach based on non-conventional laminates made of shallow bi-angle plies. We specifically employ a $\pm 25°$-ply laminate, in which the shallow-angle cross plies are bundled together in the form of non-crimped fabrics. These shallow bi-angle fabrics are axially stiff, yet they retain transverse and shear stiffness. Thus, we can create a *hard laminate* – a laminate with high axial stiffness – just by using two ply orientations, instead of using the combinations of the classical four ply orientations. Due to the reduced ply angle, we also expect relaxed stress concentration and stiffness mismatching in the shallow-angle laminates, resulting in less micro-cracking, tougher laminate, and less delamination. Additional impact of the shallow-angle laminates is easier and faster fabrication of composites. For an automated tape-laying process, for example, we can avoid four-axis lay-up by dropping single-axis bi-axial plies, which will result in significant time and cost saving [4].

Besides the shallow bi-angle approach, we also incorporate thin plies into our non-conventional laminates. With a recent development in carbon fiber tow technology, thin tows with one-third the thickness of conventional tows are made available [5]. This thinning process of the tows improves the mechanical properties of the laminates. This is because of the increased homogenization of the laminates as their ply thickness decreases. Researches have shown that benefits of the thin-ply include increased elastic modulus, tensile strength, and resistance against fatigue cycles [5, 6, 7, 8].

To demonstrate the advantage of the shallow-angle, thin-ply laminates, we first conduct coupon tests under uni-axial loading frames. Laminates composed of shallow-angle, thin plies, and conventional angle, thick plies are tested, and their performances are compared with one another to identify the benefits of the shallow-angle and thin-ply approach. Based on the findings from the coupon-level test, we design, fabricate, and test composite wing structures that employ shallow bi-angle and thin-ply laminates. We use an out-of-autoclave, vacuum assisted resin transfer molding (VARTM) method to manufacture a synergistic wing,

which employs the non-conventional laminate. The synergistic wing is composed of a sandwich panel laminate with the conventional fiber angle ($\pm 45^\circ$) for the top skin, and a sandwich panel laminate with a shallow-angle ($\pm 25^\circ$) for the bottom skin. By conducting static bending tests aided by laser Doppler vibrometry, we show the superior structural performances of the synergistic wing structure in comparison with the reference wing manufactured using conventional plies. To cross-validate the experimental results, we conduct numerical simulations aided by finite element analysis. The finite element analysis model emulates the experimental setup accurately in terms of loading and boundary conditions. The numerical results corroborate the experimental results, thereby proving the benefits of shallow-angle, thin plies in a structural application.

The manuscript is structured as follows: chapter 2 describes the coupon tests we conducted to verify the enhancement of mechanical properties of shallow-angle and thin-ply laminates. The results of coupon tests are included in chapter 2 as well. Chapter 3 presents experimental setup of structural test using test wings and the description of numerical simulation. The design, manufacturing and test setup of wings are illustrated. The results of the experiments are analyzed in chapter 4, along with the results of both experimental and simulation wing tests. Conclusion follows in chapter 5.

Chapter 2

Coupon Tests

The goal of the coupon tests is to characterize the differences between shallow ±25° bi-angle and conventional ±45° bi-angle laminates, and between thick- and thin-ply laminates. Three types of carbon fiber fabrics are tested for this purpose. Their details are tabulated in Table 2.1, and they are referred to as 'Shallow-Thin', 'Conventional-Thin', and 'Conventional-Thick' in this study, depending on their fiber orientations and ply thicknesses.

The first set of tests is conducted to assess the mechanical properties of shallow $[\pm 25]_n$ bi-angle plies. For this, laminates made with 'Shallow-Thin' and 'Conventional-Thin' fabrics are used. The thickness of one C-ply™ 25° ply is 0.125 mm, resulting in fabric thickness of 0.25 mm for ±25° non-crimped fabric (NCF). For tensile tests, four layers of the fabric are

Table 2.1: Properties of carbon fiber fabrics used in this article.

Type	Fiber Angles	Aerial Weight (g/m^2)	Fabric Product
Shallow-Thin	[±25]	300	Chomarat C-ply ™ ±25° NCF
Conventional-Thin	[±45]	150	Chomarat C-ply ™ ±45° NCF
Conventional-Thick	[±45]	410	Orca Composites ±45° NCF

laid to form $[\pm 25]_4$ laminate. Thus, the thickness of the laminate is 1.0 mm. For compressive and shear tests, $[\pm 25]_8$ and $[\pm 25]_{12}$ lay-ups are used respectively. The coupon test results will be discussed in Section A below.

The second set of tests is conducted to see the effect of thin-ply on mechanical properties of $[\pm 45]_n$ laminate. Therefore, laminates made with 'Conventional-Thin' and 'Conventional-Thick' fabrics are used. Orca Composites' $\pm 45^\circ$ NCF has individual ply thickness of 0.225 mm, and fabric thickness of 0.45 mm. C-ply^{TM}'s $\pm 45^\circ$ NCF has individual ply thickness of 0.07 mm and fabric thickness of 0.14 mm. Section B will discuss the test results.

The third set of tests is conducted to see the effect of thin-ply on mechanical properties of $[0/90]_n$ laminate. For this, laminates are made with 'Conventional-Thin' and 'Conventional-Thick' fabrics, just rotated 45° to form [0/90] fiber orientation. The test results will be discussed in Section C.

For the tensile tests of second and third sets, two layers of the Orca Composites' NCF are laid to form laminates with thickness of 0.90 mm. To achieve similar thickness, we use six layers of C-ply^{TM}'s $\pm 45^\circ$ NCF (i.e., $[\pm 45]_6$ laminate), whose thickness is 0.84 mm. In addition to the tensile testing, we perform compression and shear test on C-ply^{TM}'s $\pm 45^\circ$ laminate. For these, we use $[\pm 45]_{12}$ lay-up and $[\pm 45]_{18}$ lay-up for compression- and shear-test, respectively.

Coupons are made by first fabricating composite panels using the VARTM method. Epoxy resin (EPIKOTE MGS RIMR 135) system is used for all coupons, and the curing is done in room temperature. Next, fiberglass tabs are applied to the panels using steel epoxy (JB-weld), per ASTM standards [9, 10, 11]. Once the epoxy is cured, panels are cut into standardized dimensions (15 mm $\times$ 250 mm for tensile coupons, 10 mm $\times$ 140 mm for compressive coupons, and notched 20 mm $\times$ 76 mm for shear coupons).

All coupon tests are conducted in accordance with ASTM standards: ASTM D3039[9], ASTM D3410[10] and ASTM D5379[11] for tensile, compressive, and shear tests, respectively. The number of specimens used for each case ranges from six to fifteen. Instron 5585H serves as a testing frame. For plotting purpose, we post-process the data using locally weighted

scatterplot smoothing (loess) method. This smoothing process affects the material properties from the data by less than 0.01%.

2.1 Comparison of $[\pm 45]_n$ laminates with $[\pm 25]_n$ laminate

In Figure 2.1, we plot average $\sigma - \epsilon$ curves of tensile tests of coupons made with 'Shallow-Thin' and 'Conventional-Thin' fabrics (Table 2.1). Seven coupons are tested for each set of tests. The error bars represent standard deviations of the measured data. From the figure, it is evident that [±25] laminate has superior Young's modulus and ultimate strength, while [±45] laminate has excellent ultimate strain. The comparison of [±25] and [±45] coupons' tensile,

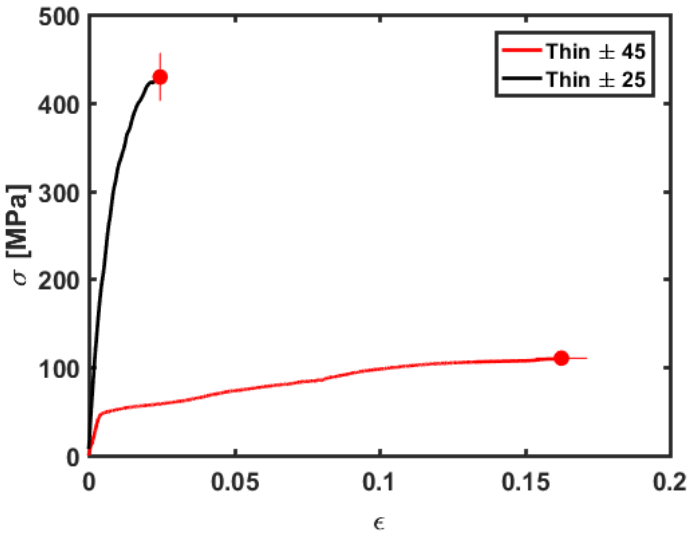

Figure 2.1: Averaged σ-ϵ curves from tensile tests of $[\pm 45]_2$, 'Conventional-Thin', coupons (red) and $[\pm 25]_6$, 'Shallow-Thin' coupons (black).

compressive, and shear test results are tabulated in Table 2.2. As fiber orientation changes from ±45° to ±25°, the laminate experiences 319.6% increase in longitudinal tensile modulus, only at a cost of 26.7% decrease in transverse tensile modulus. The case of compression is similar, with 239.5% increase in longitudinal compressive modulus and 19.1% decrease in

Table 2.2: Comparison of mechanical properties of thin-ply [±45] laminates and thin-ply shallow angle [±25] laminate.

	Thin ±45°	Thin ±25°	
	Measurements	Measurements	% deviation
E_x^+ [GPa]	12.10 ± 0.79	50.77 ± 2.82	+319.6
E_y^+ [GPa]	↑	8.87 ± 0.22	−26.7
E_x^- [GPa]	14.90 ± 1.82	50.58 ± 10.47	+239.5
E_y^- [GPa]	↑	12.05 ± 1.08	−19.1
G_{xy} [GPa]	28.29 ± 5.62	26.04 ± 4.53	−7.9

transverse compressive modulus. Noe that the shear modulus decrease from ±45° to ±25° is only 7.9%.

2.2 Comparison of thick-ply and thin-ply $[\pm 45]_n$ laminate

Figure 2.2 shows the average $\sigma-\epsilon$ curves of tensile test data of coupons made with 'Conventional-Thin' and 'Conventional-Thick' laminates (Table 2.1). 11 coupons are tested for 'Conventional-Thick' coupons, and 7 coupons are tested for 'Conventional-Thin' coupons. We can observe that while the two laminates' Young's moduli are similar, thin-ply [±45] laminate exhibits 51% higher ultimate strain $\epsilon_{x,ult}$. The ultimate strengths $\sigma_{x,ult}$ are in the similar range between the two cases. [±45] laminates demonstrate pseudo-ductility due to the scissoring of fibers[12]. The strain and stress corresponding to this pseudo-yield point, σ^y and ϵ^y respectively, are identified using 0.1% offset method[12]. This method uses the slope of the Young's modulus for a curve, offsets it from the origin by the strain of 0.1%, finds the intersection between the offset line and the original curve, and identifies it as pseudo-yield point. The

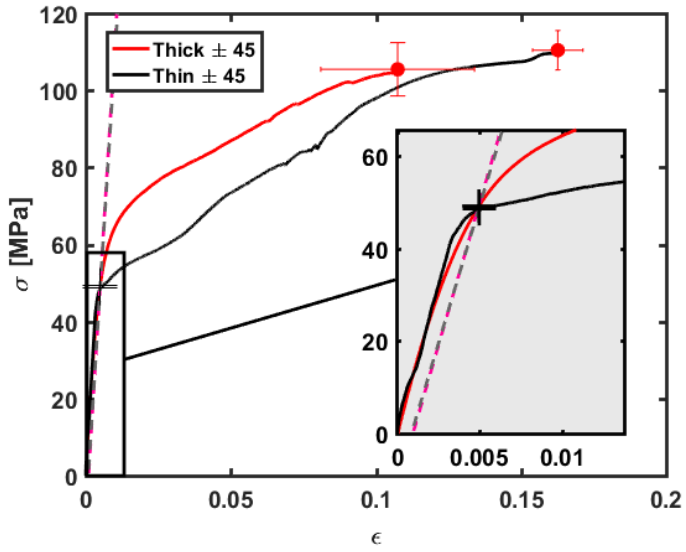

Figure 2.2: Averaged σ-ϵ curves from tensile tests of $[\pm 45]_2$, 'Conventional-Thick' coupons (red) and $[\pm 45]_6$, 'Conventional-Thin' coupons (black). Insets show the magnified view of the initial loading stage.

results of this method are visualized in the inset of Fig. 2.2. All mechanical properties, including σ^y and ϵ^y, are tabulated in Table 2.3. While thin-ply $[\pm 45]$ had improved ultimate strain, its σ^y and ϵ^y are reduced by 4.7% and 3.8% respectively. With the Young's modulus and ultimate strengths being similar between two cases, the benefit of thin-ply may not be so apparent. Thus we compare strain energies of two laminates, which will indicate the resiliency of each laminate. Strain energy is calculated by integrating the area under the stress-strain curves. The result shows thin-ply laminates retaining 49.5 % higher strain energy than thick-ply laminates before failure. This suggests laminates made with thin-ply can be significantly more resilient to elastic and non-linear deformation [13].

Table 2.3: Comparison of mechanical properties of thick- and thin-ply $[\pm 45]_n$ laminates.

	Thick $\pm 45°$	Thin $\pm 45°$	% deviation
E_x^+ [GPa]	11.84 ± 1.02	12.10 ± 0.79	+2.2
$\sigma_{x,ult}^+$ [MPa]	105.5 ± 6.9	110.4 ± 5.1	+4.6
$\epsilon_{x,ult}^+$	0.108 ± 0.027	0.163 ± 0.009	+51
Strain Energy [MJ/m^3]	9.17	13.71	+49.5
σ^y [MPa]	51.18 ± 3.59	48.76 ± 4.30	−4.7
ϵ^y	0.0053 ± 0.0002	0.0051 ± 0.0006	−3.8

2.3 Comparison of thick-ply and thin-ply $[0/90]_n$ laminate

Figure 2.3 shows the average $\sigma - \epsilon$ curves of 'Conventional-Thin' and 'Conventional-Thick' (Table 2.1) coupons, tested in $0°/90°$ fiber orientation. The effect of decreased ply thickness has a slightly different effect on $[0/90]_n$ laminates than it did on $[\pm 45]_n$ laminates. As shown in Fig. 2.3, we observe that thin ply exhibits 17.7% higher Young's modulus and 17.9% higher ultimate strain $\epsilon_{x,ult}$. Unlike the $[\pm 45]_n$ laminates, the ultimate strength $\sigma_{x,ult}$ increases by 52.8%. Values of material properties are tabulated in Table 2.4. We find that the thin-ply coupons have noticeably less deviations in Young's modulus, ultimate stress ($\sigma_{x,ult}$), and ultimate strain ($\epsilon_{x,ult}$) than the thick ply coupons as evidenced in standard deviations.

Increase in ultimate strain and strength when using thin-ply, as seen above, can be attributed to the decreased magnitude of free-edge effect. Theoretical work by Pipe and Pagano demonstrated that the magnitude of free-edge effect increases with increasing ply thickness [8]. This implies that decreasing ply thickness while keeping the laminate thickness and the ratio of the angled plies equal can decrease the magnitude of the out-of-plane shear

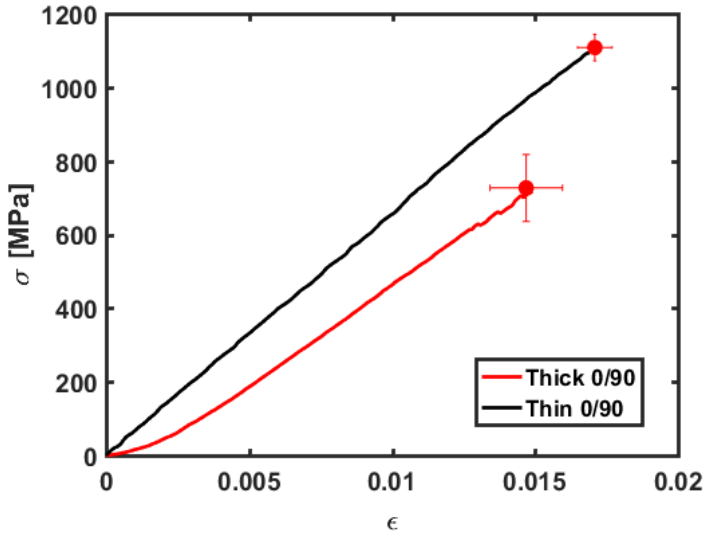

Figure 2.3: Averaged σ-ϵ curves from tensile tests of $[0/90]_2$, 'Conventional-Thick' coupons (red) and $[0/90]_6$, 'Conventional-Thin' coupons (black)

stress. More recently, Camanho *et al.* validated this effect numerically as well. In their case, changing the lay-up of $[+45_r/-45_r/0_r/90_r]_{nS}$ laminate from $r = 3, n = 2$ to $r = 1, n = 6$ effectively reduced the ply thickness by third, increasing the delamination onset strain from 2.0 % to 3.9 % [6]. More experimental results have been published recently that support this benefit [5]. In our experiments, we show that the ultimate strain increases from 10.8 % to 16.3 % for $[\pm 45]_n$ laminate, and from 1.45 % to 1.71 % for $[0/90]_n$ laminate. Our results agree with previous work of others, while it suggests that the advantageous mechanical properties

Table 2.4: Comparison of mechanical properties of thick- and thin-ply $[0/90]_n$ laminates.

	Thick 0/90°	Thin 0/90°	% deviation
E_x^+ [GPa]	55.4 ± 5.7	65.2 ± 2.2	+17.7
$\sigma_{x,ult}^+$ [MPa]	724.7 ± 91.6	1107.2 ± 36.0	+17.9
$\epsilon_{x,ult}^+$	0.0145 ± 0.0014	0.0171 ± 0.0006	+52.8

of thin-ply can depend highly on the type of lay-up.

Chapter 3

Structural Tests

In the previous section, we observed the improvement of mechanical properties of shallow-angle, thin-ply laminates in a coupon level. We now demonstrate how such advantages in the coupon test are translated into a structural level. For this, we conduct both experimental and numerical tests by using a simplified wing structure that employs combinations of conventional and shallow-angle, and thick- and thin-plies. Note that the wings fabricated in this study are far from typical composite wings, where their structural performances are optimized using complicated lamination and ply drop-off [14]. Nonetheless, we use simple lamination using a single type of fabric for each wing skin. This is to better observe the differences of structural performances between the non-conventional and the conventional laminates attributed by the change of fabric types.

We first design, manufacture, and test wing parts for experimental verifications. NACA 63-618 airfoil is chosen for the profile of our wing, considering its common usage in low speed applications. An illustration of different wing components is given in Fig. 3.1. The wing is composed of multiple sections: top and bottom sandwich panel skins, a sandwich panel shear web, and a leading edge cap. The top and bottom skins are 8.5 mm thick including 6.35 mm foam core. The thickness of the shear web is 10.5 mm, and the leading edge cap is 0.5 mm.

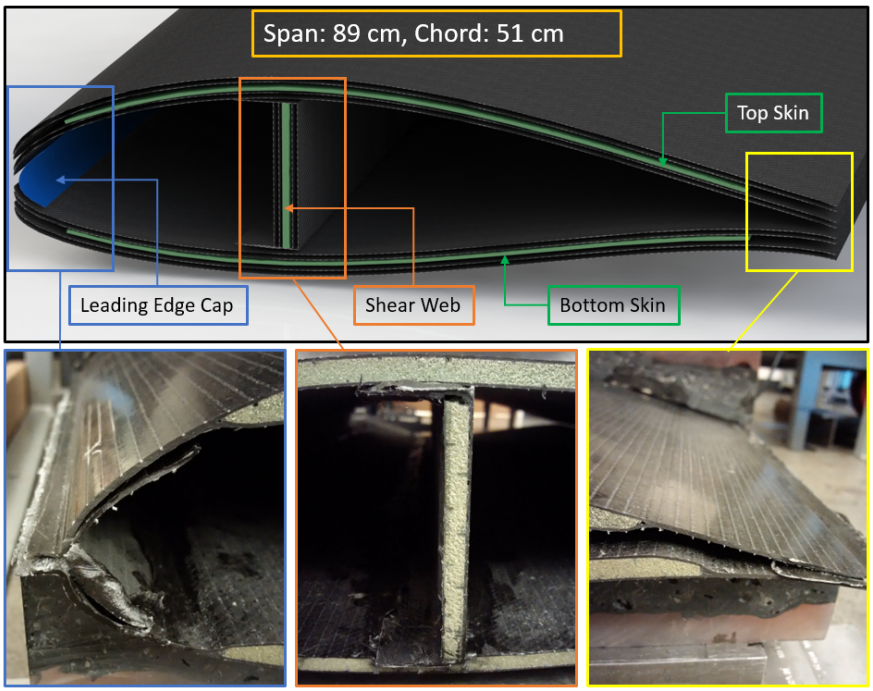

Figure 3.1: Components of the test wing. In each skin, black section denotes CFRP, while green section is foam core. Three photos below are taken from a real test wing.

Figure 3.2 outlines the manufacturing process of a wing. Here we briefly describe the manufacturing process in multiple step: (a) From the computer aided design (CAD) model, we extract the outer mold line of the top/bottom skin and the leading edge tab. (b) Computerized numerical control (CNC) router uses these profiles to cut out high-density foam (OBO Modulan 302 high density foam available through McCausey Specialty Products) into master plugs. (c) These plugs receive surface treatment including sanding, surface priming (DURATEC^{TM} 707-002), and applying of Teflon-based mold-release. They serve as templates for fiberglass molds. Fiberglass laminate is laid on master plugs with wet layup method using epoxy resin system (West System 105 Epoxy Resin and West System 209 Hardener). Once fiberglass molds are cured, (d) we surface-prepare the fiberglass molds as well, using Orange Tooling Gel Coat (Fiberflass Supply Inc.). Next two steps are part of the VARTM process for out-of-autoclave composite manufacturing approach. We start the

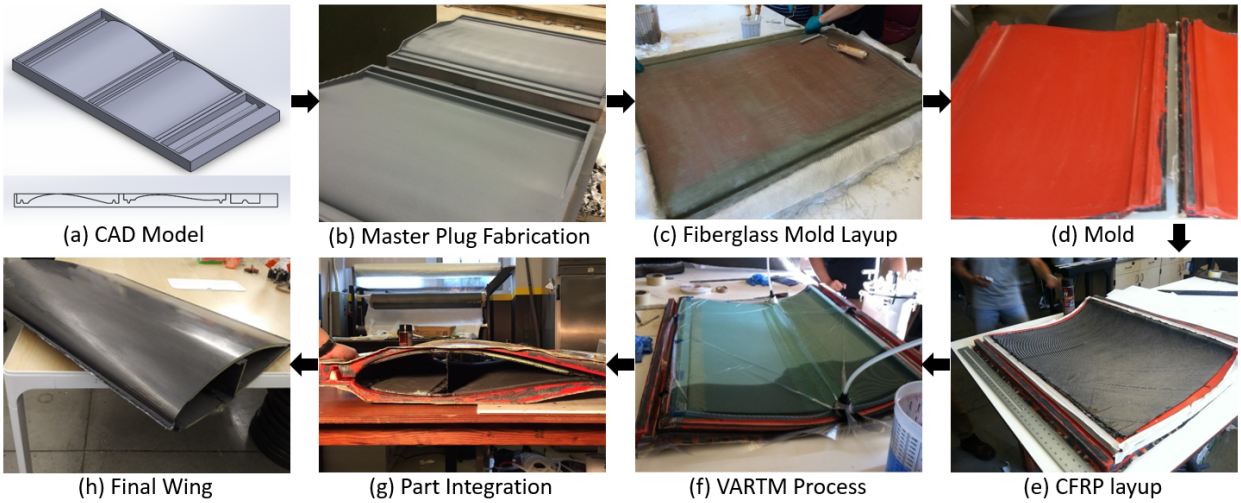

Figure 3.2: Wing manufacturing process, from design to lay-up and assembly. VARTM process is used for out-of-autoclave composite manufacturing purposes.

process by applying mold release on a mold and letting it to dry completely. (e) Next, we place the lay-up of fabrics, foam core, and resin flow mesh in a mold. (f) We bag the material and apply vacuum. We start the resin flow with an input port on one side of the wing span and output port on the other. Once enough resin has flown to wet all dry fibers, input flow is cut, continuous vacuum condition is applied to extract extra resin, and output flow is cut as well. Halogen heat lamp is placed above the setup to bring the temperature of the cure environment over 25 °C. The part is cured for at least 24 hours, after which it is released from the mold. (g) Completed parts are assembled by secondary bonding using epoxy adhesive. Photos of bonded joints can be seen in Fig. 3.1.

In this study, we fabricate three wings, and the variable among them is the type of fabric used in the skin lay-up. The first wing uses thick plies throughout the wing structure using conventional $\pm 45°$ lay-ups. The second one uses thin plies, while maintaining the same lay-up profiles. The last wing employs a synergistic wing structure, which adopts shallow-angle (i.e., $\pm 25°$), thin-skin laminate in the bottom skin of the wing. In this paper, we refer to these three test wings as Thick 45, Thin 45, and Thin 25-45 wings, respectively, as tabulated

Table 3.1: Detailed fabric composition of three test wings and their weight. Aerial weight of the fabric is denoted by gsm (gram-per-square-meter)

Wings	Top Skin	Bottom Skin	Shear Web	Weight [kg]
Thick 45	Orca Composites ±45° NCF	Orca Composites ±45° NCF	Orca Composites ±45° NCF	5.1
Thin 45	C-Ply ™ ±45° NCF	C-Ply ™ ±45° NCF	C-Ply ™ ±45° NCF	4.4
Thin 25-45	C-Ply ™ ±45° NCF	C-Ply ™ ±25° NCF	C-Ply ™ ±45° NCF	4.9

in Table 3.1 along with their lay-up. Because of different individual ply thickness of the three fabrics used, there are variations of thickness among the three wings. For example, the skin made with the thick-ply ±45° fabric is 8.2 mm thick, while the skin made with the thin-ply ±45° fabric is 8.0 mm thick. This, along with excess amount of adhesive used during the assembly, make differences in weight and stiffness, and such weight-variation effect is taken into account during analysis by normalizing stiffness values by weights.

To assess the structural performance of the wings, we conduct static bending tests. For this, test jigs are designed so that they can constrain a wing stably and load it into a bending along its span direction. The material for jigs is a polyester resin and chopped carbon fiber composite. They are cured on the same molds that are used for test wing fabrication. As a result, they have the same airfoil profile. Figure 3.3a illustrates the experimental setup. Four-point bending is chosen to keep the load stably on top of the wing. Two locations in the middle where loads are applied are 10 cm apart. Combined load of up to 285 kg is applied by incrementally stacking 20.5 kg (45 lbs) barbell plates on a flat piece of aluminum slab placed on the top of the jig. At each loading, the displacement in the middle, δ, is measured by a laser Doppler vibrometer (Polytec, OFV-505) in the resolution of $500\,\mu\mathrm{m\,V^{-1}}$. A mirror is placed under the wing to deflect the laser by 45° so that the vibrometer measures the wing's vertical displacement. Under the application of the loads, the test jig can also deform. Thus, we also measure the displacements of the both ends of the wing span using the vibrometer,

and we subtract these global deflection values from the measured central wing deflection. This way, we obtain the information of the pure deflection of the wing center.

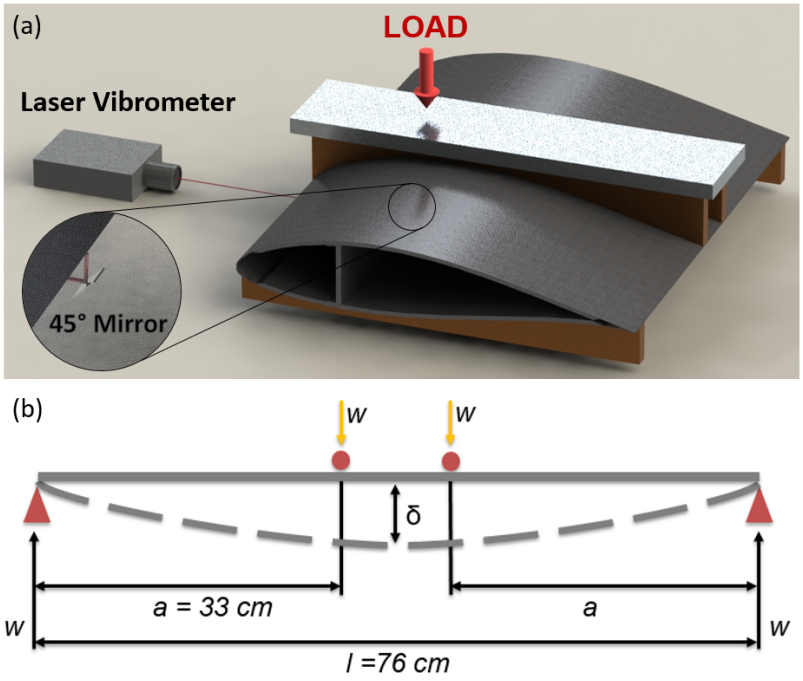

Figure 3.3: (a) A rendering of experiment setup, and (b) its analogous representation as a beam bending case.

For the comparison with the experimental results, we build a finite element analysis (FEA) model by using commercial software (ABAQUS). The CFRP material properties gained from coupon tests are used as materials properties. In the case of sandwich panel, its properties are calculated using laminate theory based on the material properties of the CFRP and foam core. The loading conditions are applied by imposing force to the model, the same way that the experiment test are carried out. We run linear perturbation solutions at increments of 20.5 kg up to 285 kg and record the vertical deflection of the node located at the center of the wing that corresponds to the experimental measurement point.

Chapter 4

Wing Test Results

In this paper we only consider span-wise bending and not chord-wise bending or torsion of test wings. The setup can be analyzed as a four-point beam bending problem, where the bending stiffness E_f can be represented by $E_f \sim \frac{W}{\delta}$, where W is the load applied and δ is the deflection measured at the center of the wing. Figure 4.1 shows the test data plotted with deflection (δ) in the x-axis and load (W) in the y-axis. Linear fits are performed on these data and their slopes noted as tabulated in Table 4.1. By comparing stiffness, one can observe that Thin 25-45 wing is stiffer than Thick 45 wing by 9.5 %, and Thin 25-45 wing by 35 %. It should be noted that this alone does not represent the effect of the skin variation fully. This is because test wings vary slightly in weight. The reasons for this are, first, slight variation in skin thickness due to different ply thickness, and second, varying amount of excess adhesive used in the assembly. Thicker skins and more adhesive add to the stiffness of the whole structure. For that reason, we deem that comparing stiffness-to-weight ratio would be a more fair comparison. Assigning a relative stiffness-to-weight ratio of 1 to Thick 45 wing and treating it as a baseline, we see that Thin 45 wing and Thin 25-45 wing are 25 % and 40 % stiffer than Thick 45 wing, respectively. This result, particularly the effect of shallow-angle plies for the Thin 25-45 prototype, is remarkable, showing a notable improvement over the conventional *black aluminum* design. We expect that the results will

Table 4.1: Comparison of stiffness of three test wings- experiments.

Wings:	Thick 45	Thin 45	Thin 25-45
Weight [kg]	5.1	4.4	4.9
Slope [kg µm^{-1}]	0.7759	0.8368	1.0464
Relative stiffness	1	1.078	1.349
Relative stiffness-to-weight Ratio	1	1.25	1.40
Improvement [%]	+0	+25	+40

be further improved if this non-conventional design had been used in both top and bottom skins.

By applying similar analysis to the load-deflection curves from our numerical simulations, we can computationally compare the span-wise bending stiffness of our wing prototypes. From the slope alone, we see that the Thin 45 wing being 1.1 % less stiff, and the Thin 25-45 wing being 50 % stiffer than the Thick 45 wing. The weights of the wings are taken from the mass properties of each model and are considered into calculation of relative stiffness-to-weight ratios. This brings the improvement of relative stiffness-to-eight ratio of Thin 45 and Thin 25-45 to 6.9 % and 39 % respectively (Table 4.2). These numerical results are in qualitative agreement with the experimental results.

Both experimental and numerical results are in line with those gained from our coupon testing. Coupon tests suggest that thin-ply does not have significant improvement in the stiffness, which is the case for Thin 45 wing when only stiffness is compared. Nonetheless, thin-ply does seem to result in the improved stiffness-to-weight ratio, 25 % in experiment and 6.9 % in simulation. In addition, we expect that thin-ply will increase the failure strength and strain of a wing greatly, though we did not conduct this failure tests in this study. The test results also prove that $\pm 25^\circ$ fabric can be used effectively in wing structures. By changing one side of the wing skin from $\pm 45^\circ$ to $\pm 25^\circ$ fiber orientation, the structure's span-wise

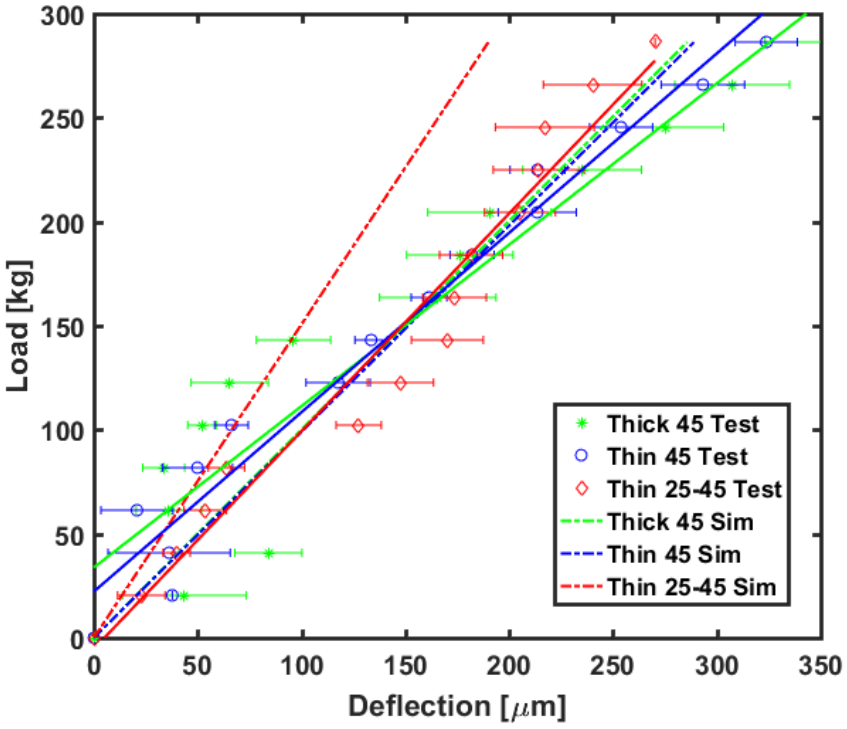

Figure 4.1: Load vs. deflection curves of experimental tests and numerical simulations. The slope ($\frac{W}{\delta}$) represents the bending stiffness of a structure.

longitudinal stiffness is increased by 40 % in experiment and 39 % in simulation.

The difference between experimental and numerical simulation results can be attributed to the inconsistent manufacturing quality introduced in the assembly of test wings. Also, our numerical model does not account for the accurate mechanical properties of adhesives. All bonding surfaces in our numerical models are assumed to form perfect bonding using tie constraints, making simulation wing structures stiffer than the real test wings with deformable adhesive in bonding surfaces.

We would like to emphasize that all fiber orientations used in our wings are achievable by one-axis lay-up. Yet we can tailor laminate properties from *soft laminate* to *hard laminate* with ease. This confirms that the non-conventional laminate introduces a new way to optimize structures in engineering applications, while reducing manufacturing time and

Table 4.2: Comparison of stiffness of three test wings- simulation.

Wings:	Thick 45	Thin 45	Thin 25-45
Weight [kg]	4.67	4.32	5.06
Slope [kg µm^{-1}]	1.003	0.9888	1.5042
Relative stiffness	1	0.989	1.504
Relative stiffness-to-weight Ratio	1	1.069	1.388
Improvement [%]	+0	+6.9	+39

complications involved. Nonetheless, one axis layup with shallow bi-angle fabrics such as $\pm 25^\circ$ will require off-axis plies to have discontinuous seams. This results in a marginal loss of laminate stiffness and approximately 20 % decrease in transverse strength in the case of $\pm 25^\circ$ fabric [4]. In addition, the drastic increase in wing bending stiffness we see in our tests will not translate to commercial wings directly, as they already use optimized lamination with much of 0° fiber along the span. However, incorporating non-conventional shallow-angle plies in their design to replace 90° and $\pm 45^\circ$ can certainly help decreasing structural weight.

Chapter 5

Conclusion

In this paper, we tested non-conventional laminates made of shallow-angle and thin plies to show their mechanical advantage above the conventional fabrics. We first conducted coupon level tests under uni-axial loading frames. We then fabricated a wing structure made of various combinations of thick-/thin- and conventional-/shallow-angle plies. According to the coupon level tests, it was evident that shallow-angle, thin-ply technology can increase failure stress and strain of a laminate by improving homogenization and reducing free-edge effect. We found that ply thickness does not have a significant effect on laminate Young's modulus. It appeared that thin-ply improves quality of a laminate to behave more consistently and predictably. Shallow bi-angle fabric introduces a new way to create *hard laminate*. Our coupon tests showed that compared to $\pm 45^\circ$ laminate, $\pm 25^\circ$ laminate had $\sim$300 % increase in axial modulus only at a cost of 25 % decrease in transverse modulus. One disadvantage of shallow bi-angle fabric is that off-axis fibers are discontinuous when multiple rows of fabric are used in a structure. This can, however, be overcome potentially by a staggering layup of bi-axial tapes. Based on the structural level test, we demonstrated that the shallow angle fabric can increase the structure's longitudinal bending stiffness significantly. Specifically, the hybrid wing composed of thin-ply $\pm 25^\circ$ and thin-ply $\pm 45^\circ$ wing had enhanced longitudinal bending stiffness than the baseline wing composed solely of thick-ply

$\pm 45°$. The improvements that were seen in experiments and simulations were both near 40 %. Manufacturers can apply non-conventional composite fabric such as shallow-angle and thin-ply technology in making composite parts. This can improve parts' structural performances, and reduce manufacturing cost and complications by negating the need for the current practice of four-axis tape lay-up.

Acknowledgments

We thank Professor Stephen Tsai at Stanford University and Professor Sung Kyu Ha at Hanyang University in Korea for helpful discussions. In addition, we thank Jesse Hartzell and Brian Laufenberg at Chomarat North America for the generous support of C-ply^{TM}materials. We acknowledge funding support from the Joint Center for Aerospace Technology Innovation (JCATI) of the Washington State. In addition, We thank Seunghyun Ko, Wei-Siang Lay, Jingmeng Tian, Paochen Chang, and Seiji Umeda Thielk for help with material fabrication and test, and Dr. Hyung-Jun Bang of Korea Institute of Energy Research for invaluable consultation regarding wing design and composite properties. The author personally thanks Professor Jinkyu Yang at University of Washington who mentored the author as an advisor, and Professor Marco Salviato at University of Washington for serving as a thesis committee member.

Contributions

This thesis was built on the work started by undergraduate students as their project in the summer of 2014. Seunghyun Ko, Wei-Siang Lay, and Paochen Chang were students in the department of Aeronautics and Astronautics Engineering, and Jingmeng Tian, and Seiji Umeda Thielk were students in the department of Materials Science and Engineering. They fabricated and established the setup required for VARTM process under the mentor-ship of Dr. Hyung-Jun Bang and Professor Jinkyu Yang. Students fabricated molds, set up vacuum infusion system, and purchased materials. During the year 2015, the students helped in fabricating three test wings. They presented their progress in a AIAA conference[16].

The author contributed in structural analysis, both experimental and simulational. His progress and intermediate findings were presented in a AIAA conference in 2016 [17].

This thesis is based on the manuscript to be submitted to AIAA by the author.

Bibliography

[1] Masuelli, M.A. Introduction of Fibre-Reinforced Polymers-Polymers and Composites: Concepts, Properties and Processes; INTECH Open Access Publisher: Rijeka, Croatia, 2013.

[2] Chung, D. Carbon Fiber Composites; Butterworth-Heinemann: Oxford, UK, 1994.

[3] Wagner, M., Norris G., "Boeing 787 Dreamliner" MBI Publishing Company, ISBN: 9781616732271, 2009

[4] Tsai, S.W., Melo, J.D.D., "Composite Materials Design and Testing," JEC Group, Stanford CA., 2015

[5] S. Sihn, R. Y. Kim, K. Kawabe, and S. W. Tsai, "Experimental studies of thin-ply laminated composites," Compos. Sci. Technol., vol. 67, no. 6, pp. 996-1008, 2007.

[6] Camanho, Pedro P., et al. "Structural Integrity of Thin-Ply Laminates," Composites Science and Technology 06/2014; 98. DOI:10.1016/j.compscitech.2014.04.014

[7] A. Arteiro, G. Catalanotti, J. Xavier, and P. P. Camanho, "Notched response of non-crimp fabric thin-ply laminates," Compos. Sci. Technol., vol. 79, pp. 97-114, 2013.

[8] Pipes, R. B., and Pagano, N. J.,"Interlaminar Stresses in Composite Laminates Under Uniform Axial Extension," J. Compos. Mater., 4 ,1970, pp. 538-548.

[9] ASTM Standard D3039/D3039M, 2014, "Standard Test Method for Tensile Properties of Polymer Matrix Composite Materials", ASTM International, West Conshohocken, PA, 2013, DOI: 10.1520/D3039_D3039M-14, www.astm.org.

[10] ASTM Standard D3410/D410M, 2008, "Standard Test Method for Compressive Properties of Polymer Matrix Composite Materials with Unsupported Gage Section by Shear Loading", ASTM International, West Conshohocken, PA, 2008, DOI: 10.1520/D3410_D3410M-03R08., www.astm.org.

[11] ASTM Standard D5379/D5379M, 2012, "Standard Test Method for Shear Properties of Polymer Matrix Composite Materials by the V-Notched Beam Method", ASTM International, West Conshohocken, PA, 2012, DOI: 10.1520/D5379_D5379M-12., www.astm.org.

[12] J. D. Fuller and M. R. Wisnom, "Pseudo-ductility and damage suppression in thin ply CFRP angle-ply laminates," Compos. Part A Appl. Sci. Manuf., vol. 69, pp. 64-71, 2015.

[13] Society of Plastics Engineers. (1980). Polymer composites. Brookfield, CT: Society of Plastics Engineers.

[14] G. J. Kennedy, and J. R. R. A. Martins, "A comparison of metallic and composite aircraft wings using aerostructural design optimization," 12th AIAA Aviation Technology, Integration, and Operations (ATIO) Conference, Indianapolis, Indiana, 17-19 September 2012.

[15] J. M. Gere and S. P. Timoshenko, "Mechanics of Materials," 3rd ed. Boston: PWS-Kent, 1990

[16] P. Chang, S. Ko, W. Lay, J. Tian, S. Thielk, N. Kimber, J. Yang, "Development of Advanced Composite Wings Using C-Ply via VARTM Process," AIAA Region VI Student Conference, Reno, NV, 2015.

[17] Y. H. N. Kim, P. Chang, S. Ko, W. Lay, J. Tian, S. Thielk, H. Bang, J. Yang, Effects of shallowangle, thin-ply laminates on the structural performance of composite wing, AIAA SciTech, 2016.